Biochem. J. (1979) **181**, 21–36
Printed in Great Britain

Crystal Structures of Hen Egg-White Lysozyme Complexes with Gadolinium(III) and Gadolinium(III)–*N*-Acetyl-D-glucosamine

By Stephen J. PERKINS,*† Louise N. JOHNSON,* Pella A. MACHIN‡ and David C. PHILLIPS*

**Laboratory of Molecular Biophysics, Department of Zoology, University of Oxford, South Parks Road, Oxford OX1 3PS, U.K., and ‡Science Research Council Daresbury Laboratory, Daresbury, Warrington, Cheshire WA4 4AD, U.K.*

(*Received* 9 *November* 1978)

Analysis at 0.25 nm resolution of the crystal structures of lysozyme–Gd(III) and lysozyme–Gd(III)–N-acetyl-D-glucosamine (GlcNAc), prepared by diffusion methods, show that there are two main binding positions for Gd(III), one of which is close to glutamic acid-35 and the other close to aspartic acid-52. The two sites are 0.36 nm apart. There is no evidence for the weak binding of Gd(III) to any of the eight other carboxy groups of lysozyme. In the presence of Gd(III), the binding of GlcNAc is similar to that observed for the binding of the β-anomer in subsite C. There are numerous small conformational changes in the protein on binding Gd(III) and the sugar, and these have been quantified to a first approximation by real-space refinement. These changes are similar in both structures, and involve, among other small movements, shifts of one of the disulphide bridges by up to 0.05 nm. The movement of residues 70–74 observed in the binary complex of lysozyme–GlcNAc [Perkins, Johnson, Machin & Phillips (1978) *Biochem. J.* **173**, 607–617] is not observed in the ternary complex of lysozyme–Gd(III)–GlcNAc. The nature of the lysozyme–Gd(III) complex is discussed in the light of evidence from other crystallographic studies and n.m.r. solution studies. Preliminary findings for a lysozyme–Gd(III) complex prepared by co-crystallization methods are reported.

The binding sites of paramagnetic metal cations in complexes with hen egg-white lysozyme are of general interest in view of the many n.m.r. studies that have been reported with these complexes (Dwek *et al.*, 1971, 1973; Dwek, 1973; Campbell *et al.*, 1975; Agresti *et al.*, 1977; Lenkinski *et al.*, 1978). From the change in relaxation times or chemical shifts in the protein or inhibitor signals, distances from the metal to the nuclei studied by n.m.r. may be calculated.

At the present stage of n.m.r. techniques, comparative studies based on the X-ray analysis of crystalline metal–lysozyme complexes are most relevant. Crystallography will not only give distances, which may be compared with those obtained in solution, but it will also reveal information about the nature of chelation of the metal to the protein. A complication of the n.m.r. studies is the possibility of non-specific weak binding of the metal to carboxy groups other than those in the major lanthanide-binding site (Campbell *et al.*, 1975). These additional sites may be detected through the use of the standard methods of difference Fourier synthesis to locate the heavy-atom positions (as reviewed in Blundell & Johnson, 1976). Further, under conditions of fast exchange, studies of binding equilibria by n.m.r. cannot establish how many sites may be competing for ligand binding, whereas crystallographic studies do so by direct observation.

Several studies of lysozyme–lanthanide and lysozyme–transition-metal complexes have been published. In a low-resolution (0.6 nm) study on the tetragonal crystal form of a lysozyme–gadolinium complex, Gd(III) was observed to bind between aspartic acid-52 and glutamic acid-35 in the catalytic site between subsites D and E (C. C. F. Blake, personal communication; Imoto *et al.*, 1972). The binding of the metal at this site naturally inhibits the enzyme activity. Extension to 0.25 nm resolution suggested two sites for Gd(III) bound to each of these carboxy groups (Perkins, 1977; Perkins *et al.*, 1976). The 0.2 nm-resolution studies on the triclinic crystal form of lysozyme (Kurachi *et al.*, 1975) have also shown two sites for Gd(III) between the carboxy groups of aspartic acid-52 and glutamic acid-35, though in these crystals they were weakly occupied. The binding of transition metals has been studied by Kurachi *et al.* (1975) and by Teichberg *et al.* (1974). In triclinic lysozyme, binding sites for Mn(II) (22% occupancy) and Co(II) (4.8% occupancy) were located about 0.25 nm from one of the oxygen atoms

Abbreviations used: GlcNAc, *N*-acetyl-D-glucosamine; αMeGlcNAc, α-methyl *N*-acetyl-D-glucosaminide; βMeGlcNAc, β-methyl *N*-acetyl-D-glucosaminide.

† Present address: European Molecular Biology Laboratory, c/o C.E.N.G., L.M.A., 85X, F-38041, Grenoble Cedex, France

of glutamic acid-35 (Kurachi *et al.*, 1975). However, a study of Cu(II) binding by using *hk*0, *h*0*l* and *hkl* projection maps in tetragonal lysozyme showed the metal-binding site to be 0.2–0.3 nm from the aspartic acid-52 carboxy group and 0.5 nm from the glutamic acid-35 carboxy group (Teichberg *et al.*, 1974).

The present paper describes the 0.25 nm-resolution crystallographic experiments for lysozyme complexes with Gd(III) and with Gd(III)–GlcNAc in the tetragonal crystal form. The metal sites were located from difference Fourier syntheses and subsequently refined by using a phased-refinement method. The shifts in the protein structure were determined to a first approximation by using real-space refinement methods.

Experimental

Preparation of crystals by diffusion

Tetragonal hen egg-white lysozyme crystals, space group $P4_32_12$, were grown in the conventional manner at pH 4.7, by using concentrations of 50–60 mg of lysozyme/ml in a solution of 5% (w/v) NaCl/40 mM-sodium acetate buffer, at room temperature. Single crystals were transferrred to a small vial with 0.5 ml of the mother liquor. The complexes with the lanthanides and inhibitor were prepared by diffusion: 0.5 ml of a $Gd(OAc)_3$ or a $Gd(OAc)_3$/GlcNAc solution was prepared in a separate portion of the mother liquor used in crystallization and added slowly, over a period of 1 h, to the solution containing the crystals, to minimize the effects of osmotic shock. Soaking periods were about 20 h. The pH of these soaking conditions was checked at a later date to ensure that the pH was approx. 4.7 or higher. Small crystals (0.3 mm × 0.3 mm × 0.3 mm or less, suitable for the preliminary precession-camera studies) generally remained clear, although larger crystals of dimensions 0.8 mm × 0.8 mm × 0.8 mm (used for the 0.25 nm-data collection) tended to dissolve slightly or crack in solutions of higher $Gd(OAc)_3$ concentration. Preliminary work suggested that too high a GlcNAc concentration [50 mM-$Gd(OAc)_3$/250 mM-GlcNAc] inhibited the binding of Gd(III). The concentrations used in the 0.25 nm-data collection after the testing of several Gd(III) and GlcNAc concentrations by using precession photographs were 50 mM-$Gd(OAc)_3$ and 33 mM-$Gd(OAc)_3$/67 mM-GlcNAc. Single crystals of the lysozyme complexes were transferred to quartz capillary tubes, the mother liquor was drawn off gently, and the capillaries were sealed in the usual manner.

Preparation of crystals by co-crystallization

Experience from the n.m.r. studies showed that lysozyme is soluble in concentrations of lanthanides equivalent in ionic strength to those used for crystallization with 4–5% NaCl. Further, the presence of acetate anion is known to affect the affinity of lysozyme for Gd(III) (Jones *et al.*, 1974). Thus an attempt was made to crystallize acetate-free lysozyme (prepared as described in Perkins, 1977) in the presence of NaCl and $GdCl_3$ alone. $GdCl_3$ solution (1 M) was prepared by heating the oxide in a slight excess of HCl and subsequently neutralizing with NaOH.

The crystallization of lysozyme–Gd(III) crystals was most successful with 200 mM-$GdCl_3$/10% (w/v) NaCl and 75 mg of lysozyme/ml at pH 5.0–5.2. The use of other Gd(III) concentrations resulted in the appearance of spheruloids (amorphous semi-crystalline assemblies). The lysozyme–Gd(III) crystals are tetragonal and are fragile, being cleaved easily.

Data collection

X-ray-diffraction data in the resolution range 0.8–0.25 nm were collected on a Hilger and Watts linear diffractometer modified to measure five reflexions simultaneously (Phillips, 1964; Arndt *et al.*, 1964) by using a Philips fine-focus X-ray tube with the generator run at 40 kV and 16 mA. The source-to-crystal distance was 150 mm. The crystal was mounted with the crystallographic axis a^* parallel to the rotation axis. The crystal-to-counter distance was adjusted to 365 mm in order to measure simultaneously five reflexions, with the separation of the counters 7.5 mm, and the counter arm was filled with helium. An oscillation range of 1°45′ was used. The low-resolution data and absorption curves were measured on a four-circle diffractometer.

Three crystals were used, all prepared by diffusion methods: (A) lysozyme–Gd(III) ($a = b = 7.83$ nm, $c = 3.79$ nm) (levels $h = 0$–9); (B) lysozyme–Gd(III) ($a = b = 7.87$ nm, $c = 3.79$ nm) (levels $h = 10$–19); (C) lysozyme–Gd(III)–GlcNAc ($a = b = 7.87$ nm, $c = 3.82$ nm) (levels $h = 0$–19) The unit-cell dimensions were only slightly different from those for native lysozyme ($a = b = 7.91$ nm, $c = 3.79$ nm). The relative absorption curve calculated from the variation in intensity of the strong axial 800 reflexion (North *et al.*, 1968) varied in the ranges (A) 1.00–1.78, (B) 1.00–1.81 and (C) 1.00–1.92. Radiation damage was monitored by using the changes in intensity of the 080 and 008 reflexions measured at regular intervals during the data collection. These were found to be (A) 21% decrease, (B) 14% decrease and (C) 4% decrease, During data collection, each reflexion was measured up to four times in a quarter-sphere of reciprocal space.

Data processing

The diffractometer data for all three crystals were corrected for background, Lorentz, polarization and

absorption factors (North, 1965; North *et al.*, 1968), and a linear correction was applied for radiation damage. An analysis of the agreement of the Friedel pairs was made, and an empirical correction was subsequently applied. The level scale factors for each counter were calculated from the equivalent reflexions in different levels of reciprocal space, by using a least-squares analysis (Hamilton *et al.*, 1965). The merging R values were found to be 8% for (A) and (B) and 6% for (C), where:

$$R_m = \frac{\sum_h \sum_{i=1}^{n} |\bar{I}(h) - I(h)_i|}{\sum_h \sum_{i=1}^{n} I(h)_i}$$

where $I(h)_i$ is the ith measurement of the intensity of reflexion h after scaling and $\bar{I}(h)$ is the mean value of the n measurements of the reflexion. The data were scaled to the basic native set (Blake *et al.*, 1965). The fractional change in structure factor amplitude is 0.282 for samples (A) and (B) and 0.220 for sample (C). The mean isomorphous difference is 108 for sample (A) and (B) and 86 for sample (C). Difference Fourier syntheses were computed by using coefficients $m(F_{PI}-F_P)\exp i\alpha_{iso}$, where F_{PI} and F_P are the structure factor amplitudes for the protein plus inhibitor and native protein respectively and m and α_{iso} are figure of merit and phases for the native protein respectively, which have been determined by the multiple heavy-atom isomorphous-replacement method (Blake *et al.*, 1965).

Refinement

The positions of the Gd(III) sites were found from the difference Fourier synthesis and were refined by using least-squares phased-refinement methods combined with double-difference maps (Blundell & Johnson, 1976, and references cited therein), where the phases used were those determined in the multiple isomorphous-replacement method. Initially only those reflexions for which the figure of merit of the phase determination was better than 0.80 were used. Restricting the reflexions to those for which $m>0.90$ did not lead to any significant differences in the refinement.

Preliminary work on the refinement of hen egg-white lysozyme in the tetragonal crystal form has been completed (D. E. P. Grace & D. C. Phillips, unpublished work). However, in advance of further studies, it seemed worth while to make some attempt to describe the conformational changes that occur in lysozyme on binding Gd(III) and GlcNAc. Accordingly the atomic positions of the protein and inhibitor have been refined by real-space refinement (Diamond, 1971, 1974) with a Fourier synthesis based on coefficients $m(2F_{PI}-F_P)\exp i\alpha_{iso}$ for acentric data and $mF_{PI}\exp i\alpha_{iso}$ for centric data. The calculations were carried out on the Science Research Council Rutherford Computing Laboratory's IBM 370/195 computer. The structure of lysozyme has already been refined by this method by using the isomorphous phases to yield a set of protein co-ordinates termed RS5D (Diamond, 1974). By using the same parameters (Table 1) and the RS5D co-ordinates as starting co-ordinates, relative movements of atoms can be defined with respect to this system. Clearly this represents a first approximation to a more detailed refinement, which can be made with greater ease once the refinement of the native-crystal structure is completed. During the real-space refinement the gadolinium atoms were not allowed to move from their positions determined in the phased refinement.

Results

Position of Gd(III) in the difference Fourier syntheses for lysozyme Gd(III) and lysozyme–Gd(III)–GlcNAc complexes

Figs. 1(*a*) and 1(*b*) show the two sections of the difference Fourier syntheses for the lysozyme–

Table 1. *Specification of the real-space refinement programme* (*Diamond*, 1974)

Zone length	5
Margin width	8
Fixed radius of all atoms	1.5
Relative weights of C:N:O:S:Gd(1):Gd(2)	6:7:8:16:14.7:24.3
Parametric constants of dihedral angles	
ϕ, ψ (main chain)	3.7
χ_1–χ_4 (side chain)	3.2
τ (N_i, C_i^α, C_i)	0.33
ω (main-chain peptide)	0.5
χ_5 (arginine)	0.25
$\theta_{1,2,3}$ (proline)	0.1
τ (cystine)	0.33
Filter ratio for translational rotational and weight refinement parameters	0.01

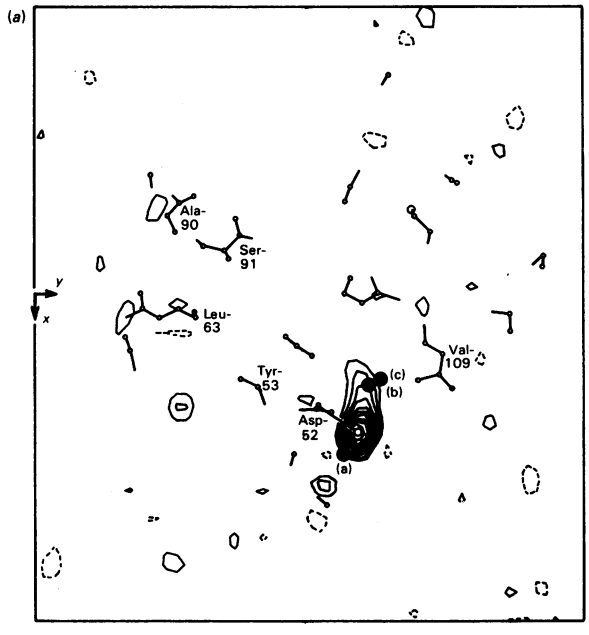
(a)
Ala-
90
Ser-
91
Leu-
63
Tyr-
53
Asp-
52
(a)
(b)
(c)
Val-
109
y
x

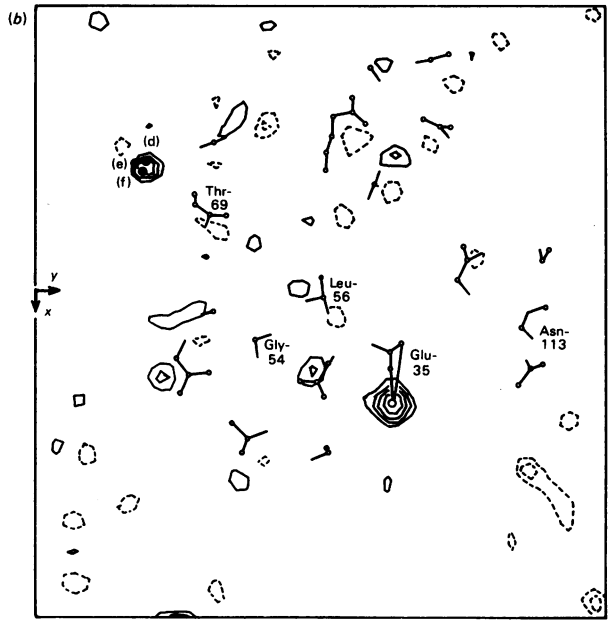
(b)
(d)
(e)
(f)
Thr-
69
Leu-
56
Gly-
54
Glu-
35
Asn-
113
y
x

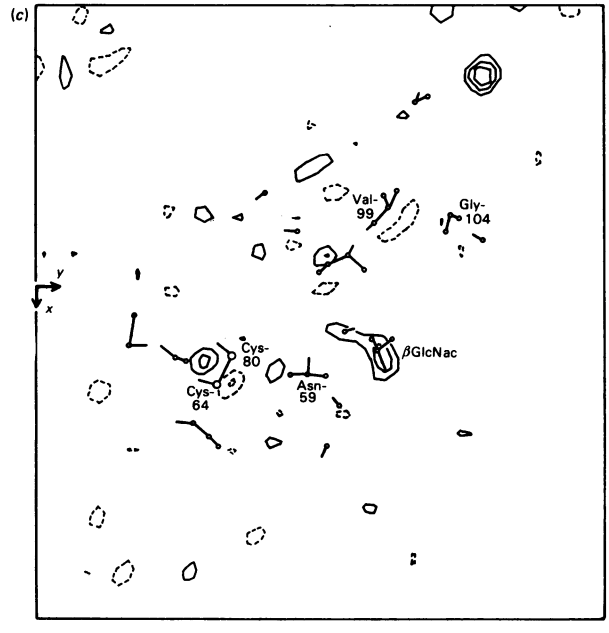
(c)
Val-
99
Gly-
104
y
x
Cys-
80
βGlcNac
Cys-
64
Asn-
59

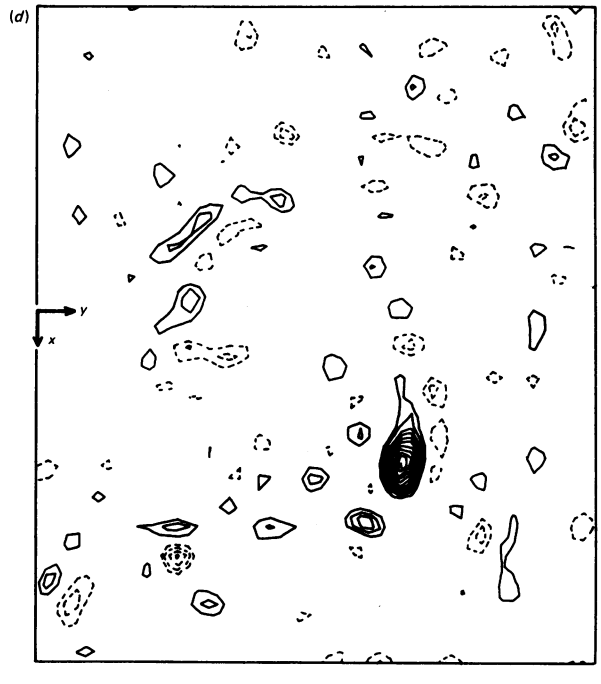
(d)
y
x

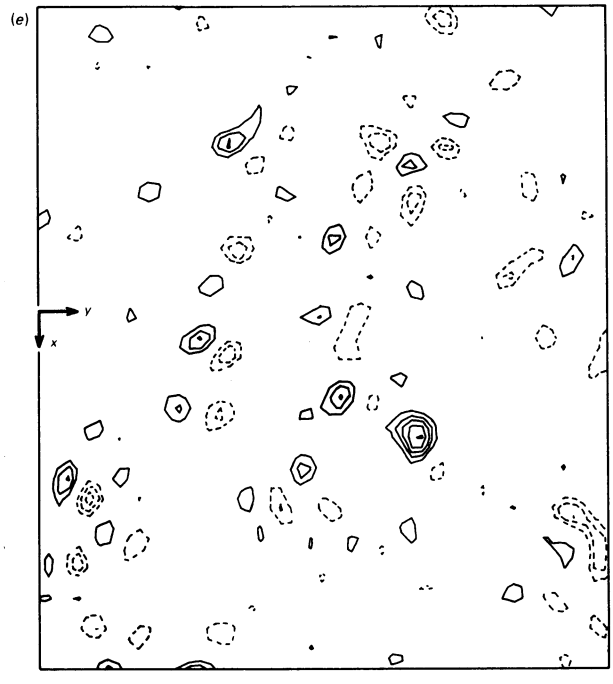
(e)
y
x

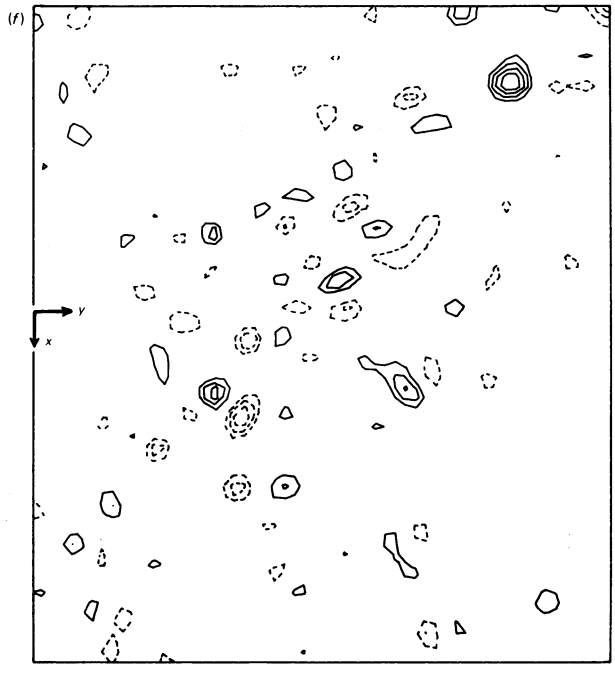
(f)
y
x

Gd(III)–GlcNAc complex in which the most intense features appear.

The two major peaks are adjacent to the carboxy groups of glutamic acid-35 and aspartic acid-52, the two catalytic carboxy groups between subsites D and E in the active-site cleft of lysozyme. The glutamic acid-35 site is weak and appears to be spherically symmetrical, whereas the aspartic acid-52 site is stronger and is associated with a residual density that tails off into the internal part of the cleft. Between these two major sites, there is continuous electron density that has a maximum of 11 contour levels (one contour level = 0.2×10^{-3} e/nm^3 at the aspartic acid-52 site and at a minimum of three contour levels in sections 31 and 30. This might be compared in appearance to an hour-glass of length 0.6nm diameter, with 0.4nm at each end and with a waist of 0.2nm diameter.

In the phased refinement, when the thermal, occupancy and three positional parameters were allowed to vary in the conventional manner, the 'Kraut' R factor as defined by:

$$R_K = \frac{\sum |F_{PI(obs.)} - F_{PI(calc.)}|}{\sum F_{PI(obs.)}}$$

improved from 0.271 to 0.251 for lysozyme–Gd(III) and from 0.211 to 0.195 for lysozyme–Gd(III)–GlcNAc on the use of two positions Gd(1) and Gd(2). At this stage the double-difference maps revealed two low-intensity lobes of positive density 0.34nm apart surrounding a clear region in the centre at the aspartic acid-52–Gd(2) site.

In order to take the 'tail' into full consideration, a subsite Gd(2B) was postulated to be adjacent to the aspartic acid-52 site. In subsequent refinement the R_K factor improved only slightly [to 0.249 for lysozyme–Gd(III) and to 0.194 for lysozyme–Gd(III)–GlcNAc]. The aspartic acid-52 site Gd(2) underwent a negligible shift of 0.01–0.03nm, and the double-difference Fourier synthesis showed no features. The errors in the refinement parameters as defined by the least-squares convergence analysis are at the most ±0.017nm for the positions of the two major sites; the errors in temperature factors and occupancies are ±10% and ±4% respectively. The results are given in Table 2.

When the multiple isomorphous-replacement phases are used, a fourth feature is visible between

Fig. 1. *Sections of the difference Fourier synthesis for the lysozyme–Gd(III)–GlcNAc complex*

(*a*)–(*c*) were calculated by using isomorphous phases, and (*d*)–(*f*) by using calculated phases. (*a*) Section 34/60: the Gd(2) site at aspartic acid-52. The positions of (a) $UO_2(OH)_n$(5), (b) $UO_2(OH)_n$(2) (section 32) and (c) UO_2F_5(1) (section 32) as used in the multiple isomorphous replacement method are shown. (*b*) Section 29/60: the Gd(1) site at glutamic acid-35. The upper left corner shows the heavy-metal 'ghost' appearing between histidine-15 and aspartic acid-52; the positions of (d) $UO_2(OH)_n$(1), (e) $UO_2(OH)_n$(4) and (f) UO_2F_5(2) are shown to coincide in position with this peak. (*c*) Section 42/60: movement of the sulphur atoms of Cys-64(S)-Cys-80(S). The positive density in the upper right corner is part of the symmetry related Gd(1) site; the positive density in the centre is part of the GlcNAc sugar, showing C-1, C-2 and C-3 together with the nitrogen and carbonyl oxygen atoms of the *N*-acetyl group. (*d*) Section 34/60 as for (*a*), but with calculated phases. (*e*) Section 29/60 as for (*b*), but with calculated phases. (*f*) Section 42/60 as for (*c*), but with calculated phases.

Table 2. *Refined positions in $P4_32_12$ symmetry of the Gd(III) sites*

Refinement parameters for site Gd(4) were obtained by using one further refinement cycle than the one used for presentation of the data above for sites Gd(1), Gd(2) and Gd(2B). Sites Gd(2B) and Gd(4) are probably spurious.

	Gd(III)–lysozyme				Gd(III)–GlcNAc–lysozyme				
	Co-ordinates		Occupancy		Co-ordinates		Occupancy		
Gd(III) site	(fractional)	(nm)	(%)	B	(fractional)	(nm)	(%)	B	Environment
Gd(1)	x 0.1034	0.818			0.1061	0.839			
	y 0.3089	2.443	24	28	0.3123	2.470	23	27	Glu-35
	z 0.4865	1.844			0.4854	1.840			
Gd(2)	x 0.1276	1.009			0.1309	1.035			
	y 0.3005	2.377	38	23	0.3007	2.379	38	21	Asp-52
	z 0.5616	2.129			0.5664	2.147			
Gd(2B) subsite	x 0.1015				0.1019				
	y 0.3035		21	25	0.3078		12	26	Asp-52
	z 0.5730				0.5725				
Gd(4)	x 0.9019				0.8927				
	y 0.0969		10	3	0.1044		6	–17	Asp-87
	z 0.4551				0.4564				His-15

histidine-15 and aspartic acid-87 in the difference Fourier syntheses. Consideration of this feature in the phased refinement (Table 2) shows that it is associated with low occupancies and with anomalous temperature factors. R_K decreased to 0.242 [lysozyme–Gd(III)] and to 0.186 [lysozyme–Gd(III)–GlcNAc].

Sites Gd(4) and Gd(2B) are similar to those used for the heavy atoms in the multiple isomorphous-replacement determination of the phases (cf. Table 2 and Table 3). The electron density of site Gd(4) is greater in the crystal with the more severe radiation damage. It is thus possible that these two features arise from the presence of heavy-metal 'ghosts', as marked in Figs. 1(*a*) and 1(*b*). This was confirmed by the calculation of a difference Fourier synthesis based on a set of calculated phases (termed SF7) that were obtained during the current refinement of the lysozyme structure in the tetragonal crystal form (D. E. P. Grace & D. C. Phillips, unpublished work). At this stage in the refinement some 40 water molecules had been placed and the conventional R value ($R = \sum |F_o - F_c| / \sum F_o$) was 0.26. In the difference map based on these calculated phases (Figs. 1*d*, 1*e* and 1*f*) the aspartic acid-87/histidine-15 site disappeared and the aspartic acid-52 subsite Gd(2B) was weaker. Sites Gd(1) and Gd(2) remained unchanged. Thus the two major features may be assigned conclusively as real gadolinium-binding sites with the suggestion of some anisotropic vibration in the aspartic acid-52 site.

The co-ordinates of sites Gd(1) and Gd(2) are reported in Table 2. Their positions are very similar in the two complexes lysozyme–Gd(III) and lysozyme–Gd(III)–GlcNAc, and give confidence in the results of the analyses despite the small improvement in R in the phased refinement.

As a comparison, least-squares refinement by using the centric terms alone was also carried out. The metal co-ordinates were found to be within 0.02 nm of those calculated by using the phased-refinement method. The temperature factors are decreased to 9 ± 4 and 2 ± 2 and the occupancies are increased to $49 \pm 3\%$ and $80 \pm 3\%$ respectively for sites Gd(1) and Gd(2) in the lysozyme–Gd(III) com-

Table 3. *Heavy-atom sites in tetragonal lysozyme crystals*

Fractional cell co-ordinates in $P4_32_12$ symmetry of the heavy-metal sites used in the determination of the multiple isomorphous replacement phases for hen egg-white lysozyme (from Blake *et al.*, 1965), their environment in the protein and their appearance in the lysozyme Gd(III)–GlcNAc difference Fourier synthesis are shown. Numbers in parentheses refer to the numbers that identify the sites. Abbreviation used: MHTS, *o*-mercurihydroxytoluene-*p*-sulphonic acid.

Site	Fractional cell co-ordinates	Occupancy (%)	B	Environment	10^{-3} × Density at site in lysozyme–Gd(III)–GlcNAc difference Fourier (e/nm^3)
MHTS(1)	*x* 0.7932 *y* 0.3862 *z* 0.4493	39.2	17.8	(Hg) Ser-24	1.0
MHTS(2)	*x* 0.7585 *y* 0.3607 *z* 0.5674	8.8	14.9	(S) Tyr-20	0.2
UO_2F_5(1)	*x* 0.0849 *y* 0.3217 *z* 0.5296	55.5	21.0	Asp-52	?
UO_2F_5(2)	*x* 0.8976 *y* 0.0974 *z* 0.4650	29.3	24.2	Asp-87 His-15	0.8
$UO_2(OH)_n$(1)	*x* 0.8938 *y* 0.0961 *z* 0.4664	47.1	19.2	Asp-87 His-15	0.8
$UO_2(OH)_n$(2)	*x* 0.0901 *y* 0.3102 *z* 0.5332	42.1	124.8	Asp-52	?
$UO_2(OH)_n$(3)	*x* 0.2266 *y* 0.4554 *z* 0.6985	9.0	190.2		0.0
$UO_2(OH)_n$(4)	*x* 0.8976 *y* 0.0869 *z* 0.4856	11.4	68.4	Asp-87 His-15	
$UO_2(OH)_n$(5)	*x* 0.1388 *y* 0.2976 *z* 0.5719	28.6	42.8	Asp-52	?

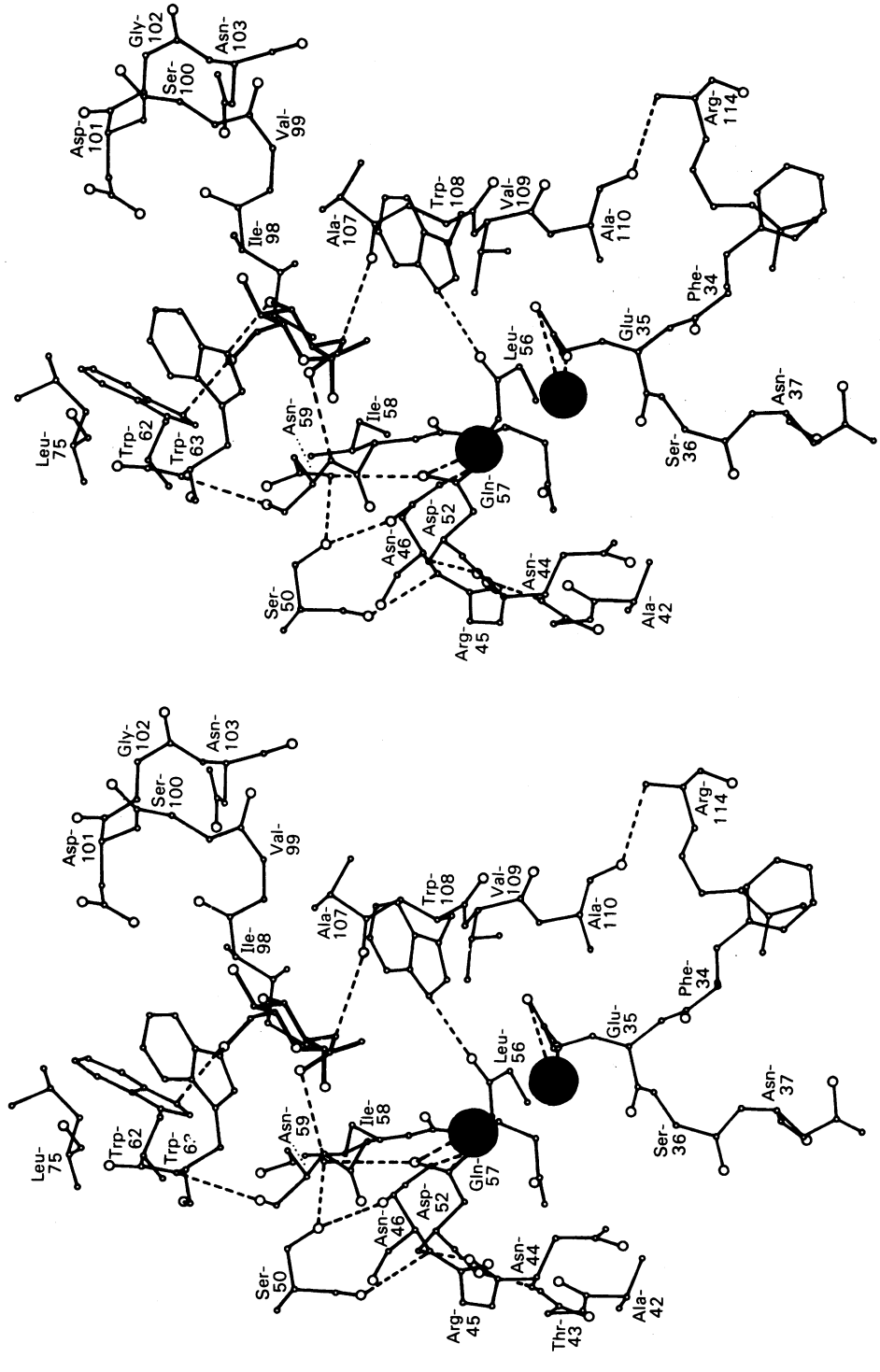

Fig. 2. *Stereo diagram of the Gd(III) sites in the active-site cleft of lysozyme, with the inhibitor GlcNAc molecule in site C*

plex. The Kraut R factor decreased from 0.357 to 0.233 and the final centric R factor was 0.702. The double-difference Fourier maps were most confused, and this is attributed to the conformational movements in the protein. These movements in the protein suggest this metal would not have formed a useful heavy-atom derivative for phase determination by multiple isomorphous replacement.

The previous 0.6nm studies on binding of gadolinium to hen egg-white lysozyme (C. C. F. Blake, personal communication) had been carried out with the $Gd(NO_3)_3$ salt. A single peak was observed in the difference Fourier synthesis with a maximum at position $x = 0.99$nm, $y = 2.37$nm and $z = 2.18$nm and elongated approx. 0.6nm in the z direction. The 0.6nm-resolution difference Fourier synthesis calculated from the present data for the lysozyme–$Gd(OAc)_3$ complex gave a very similar result, with a peak maximum at $x = 1.02$nm, $y = 2.41$nm and $z = 2.08$ nm. A more detailed comparison of the difference Fourier syntheses, however, suggests that in the lysozyme–$Gd(NO_3)_3$ complex the Gd(2) (i.e. the site closest to aspartic acid-52) is more highly occupied relative to the Gd(1) site than in the present lysozyme–$Gd(OAc)_3$ complex.

Position of the inhibitor in the difference Fourier synthesis for lysozyme–Gd(III)–GlcNAc

The difference Fourier map for lysozyme–Gd(III)–GlcNAc shows clearly that the sugar inhibitor binds only in the sugar subsite C-β in the active-site cleft (Fig. 2) in the presence of Gd(III), and not in both subsites C-β and C-α as is observed with the lysozyme–GlcNAc complex. Comparison of subsite C-α in the lysozyme–GlcNAc complex with the Gd(III) site shows that the two sites overlap to some extent: the C-6 and O-6 atoms of the sugar in subsite C-α are almost coincident with the Gd(III)-binding site Gd(2) at aspartic acid-52. The occupancy of the sugar in subsite C-β in the lysozyme–Gd(III)–GlcNAc complex is about one-third less than that observed in the lysozyme–GlcNAc complex. This may be partly explained by the lower concentration of GlcNAc used in the present study (67mM). Higher concentrations such as those used in the earlier study (500mM-GlcNAc) inhibited the binding of Gd(III), as found also by n.m.r.

Real-space refinements

Main-chain conformation. The root-mean-square movements of all atoms with respect to the RS5D lysozyme co-ordinates (Diamond, 1974) were 0.048nm for the lysozyme–Gd(III) complex and 0.045nm for the lysozyme–Gd(III)–GlcNAc complex. Both values are significantly larger than that obtained for the lysozyme–βMeGlcNAc refinement (0.036nm) (Perkins *et al.*, 1978). The movements of the main-chain α-carbon atoms are summarized in Figs. 3(*a*) and 3(*b*). These plots suggest a background value of about 0.02nm, above which positional changes may be taken as significant.

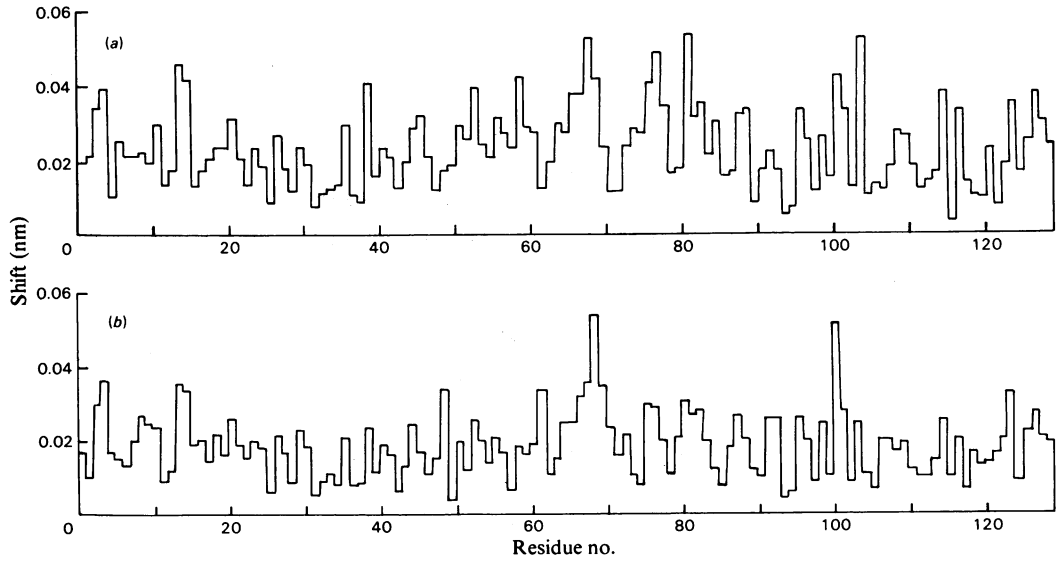

Fig. 3. *Histograms to show the movement in nm of the α-carbon atoms in lysoyzme after the first cycle of real-space refinement for (a) lysozyme–Gd(III) and (b) lysozyme–Gd(III)–GlcNAc*

It is noteworthy that the characteristic conformational movements detected in lysozyme–GlcNAc and lysozyme–βMeGlcNAc complexes for residues 70–75, which lead to a sideways movement of this loop towards the active-site cleft (Perkins *et al.*, 1978), are not observed in the lysozyme–Gd(III) or lysozyme –Gd(III)–GlcNAc complexes, although some movement at cysteine-76 is observed for the gadolinium derivative. The absence of movement in the Gd(III) complexes is confirmed by the difference Fourier syntheses, which show no features in the region of residues 70–75. It appears that movement of this loop is not essential for binding GlcNAc to lysozyme.

There are six segments of α-helix in lysozyme (Imoto *et al.*, 1972). From the difference maps, there appears relatively little systematic change in the α-helices 88–99 and 108–116, but α-helices 4–15, 24–37 and 79–84 and the β-pleated sheet at residues 42–60 shift significantly. In particular a movement of the aromatic ring of tyrosine-53 on the β-pleated sheet of about 0.03 nm is clearly visible in the difference map. No explanation of these changes appears obvious at the present time, though the change of the mother liquor from 0.9 M to 1.2 M may be influential in addition to a series of conformational movements triggered by the binding of Gd(III) in the catalytic site.

In an initial run of the real-space refinement, the α-carbon atom of arginine-21 was found to move 0.16 nm, although no indication of a large shift was apparent in the difference Fourier synthesis. Arginine-21 is close to glutamic acid-35 in a symmetry-related molecule, and inspection of the electron-density map showed that the two terminal nitrogen atoms of arginine-21 had moved by 0.5–0.6 nm into the relatively intense electron density of the glutamic acid-35 Gd(1) site of a neighbouring molecule. In the refinements reported in the present paper no rotations corresponding to χ_2, χ_3, χ_4 and χ_5 were allowed for arginine-21 and this prevented the spurious movement of this side chain.

Side chains and active-site conformation. The discussion from here on refers to the results of the real-space refinement for the lysozyme–Gd(III)–GlcNAc complex. The difference Fourier synthesis shows many conformational movements in the protein. An overall qualitative description may be based on the movements of the eight sulphur atoms involved in the four disulphide bridges, and the movements of the α-helices and the β-pleated sheet as in the difference map (Table 4). The movement of cysteine-64(S)–cysteine-80(S) is clearly visible in the lysozyme–Gd(III)–GlcNAc difference map (Fig. 1*c*). Movements are observed for the two tryptophan residues (at positions 62 and 63) which are involved in hydrogen-bond interactions through their $N^{\varepsilon 1}$ atoms to O-3 and O-6 atoms respectively of GlcNAc in subsite C-β (Table 4). In the difference Fourier synthesis for lysozyme–Gd(III)–GlcNAc there are clear indications for the movement of tryptophan-63, and these features are very similar to those observed in the lysozyme–βMeGlcNAc complex (Perkins *et al.*, 1978). However, the features representing movement of tryptophan-62 are considerably weaker than those observed in the lysozyme–sugar complex. In the native structure of lysozyme, tryptophan-62 has some mobility and becomes more firmly located in the lysozyme–βMeGlcNAc complex. In the ternary lysozyme–Gd(III)–GlcNAc complex the localization of tryptophan-62 appears to be intermediate between the native and the binary sugar complex.

Table 4. *Shifts in some side-chain atoms in the lysozyme–Gd(III)–GlcNAc complex*

Residue and atom		Shift (nm)
Cys-6(S)–Cys-127(S)		0.028, 0.046
Cys-30(S)–Cys-115(S)		0.023, 0.015
Cys-64(S)–Cys-80(S)		0.023, 0.034
Cys-76(S)–Cys-94(S)		0.023, 0.040
Trp-62	$C^{\zeta 3}$	0.057
	$N^{\varepsilon 1}$	0.054
Trp-63	$C^{\zeta 3}$	0.011
	$N^{\varepsilon 1}$	0.037
Trp-108	$N^{\varepsilon 1}$	0.030
Glu-35	C^{δ}	0.023
	$O^{\varepsilon 1}$	0.030
	$O^{\varepsilon 2}$	0.037
Asp-52	C^{γ}	0.028
	$O^{\delta 1}$	0.050
	$O^{\delta 2}$	0.037

The distance between the peptide nitrogen atom of residue 59 and the carbonyl oxygen atom of residue 107 in the acetamido specificity site is 0.76 nm in both the lysozyme–Gd(III) and lysozyme–Gd(III)–GlcNAc structure. This value is almost identical with the separation of these atoms in the native (RS5D coordinates) and the lysozyme–α/βGlcNAc complex, where the separation is 0.77 nm in both structures. The constancy of this separation of the two protein atoms that are involved in hydrogen bonds to the oxygen and nitrogen atoms respectively of the acetamido group of GlcNAc in subsite C is of significance in view of the important role of these interactions in determining the specificity for inhibitor and substrate binding.

On binding Gd(III) some movement is observed for the two carboxy groups (glutamic acid-35 and aspartic acid-52) at the catalytic site of lysozyme (Table 4). The separations of key atoms are summarized as follows in Table 5. Thus the small relative movements between aspartic acid-52 and glutamic acid-35 and between tryptophan-108 and glutamic acid-35 are of the same order of magnitude as the estimated precision (~0.02 nm) of the real-space refinement. In the native structure the $O^{\delta 1}$ atom of

aspartic acid-52 is hydrogen-bonded to the side chains of asparagine-46 and asparagine-59, where the hydrogen-bonded lengths are 0.30 and 0.27nm respectively. On movement of the carboxy group in the lysozyme–Gd(III)–GlcNAc complex these distances become 0.36 and 0.30nm respectively. Evidently the ionic interaction of the $O^{\delta 2}$ atom with the gadolinium cation causes a movement of aspartic acid-52 that weakens these hydrogen bonds.

The Gd(III)–oxygen bond lengths determined from the real-space refinement for glutamic acid-35 $O^{\varepsilon 1}$–Gd(1) and aspartic acid-52 $O^{\delta 2}$–Gd(2) are 0.26 and 0.25nm and are close to the metal–oxygen distances of 0.22–0.24nm given by Levine *et al.* (1974) and Levine & Williams (1975). The separation of the metal from the other oxygen atom of each of the carboxy groups is at least 0.35nm (Table 6). This suggests a scheme of monodentate binding of Gd(III) to aspartic acid-52 and glutamic acid-35 as shown in Fig. 2.

Sugar. Comparison of the results of the real-space refinement for the lysozyme–βMeGlcNAc (Perkins *et al.*, 1978) and lysozyme–Gd(III)–GlcNAc complexes shows that the positions of the sugars in subsite C-β are identical within 0.01 nm for the sugar ring atoms, but differ by as much as 0.1 nm for atoms of the acetamido side chain. Inspection of the difference Fourier synthesis for the lysozyme–Gd(III)–GlcNAc complex shows that there is a definite lobe of density representing the O-7 atom, which is not so distinct in the lysozyme–βMeGlcNAc complex. The real-space refinement programme has fitted the acetamido side chain to this density by a rotation of −22° about the C-2–N-2 bond from the orientation observed in the crystal structure of αGlcNAc (Johnson, 1966). The rotation observed in the lysozyme–βMeGlcNAc study was +12% (Perkins *et al.*, 1978). In spite of the relatively large rotational differences between the acetamido group in the two complexes, the hydrogen-bond length from O-7 to the N atom of asparagine-59 does not change significantly [0.33nm in lysozyme–βMeGlcNAc and 0.34nm in lysozyme–Gd(III)–GlcNAc], although in lysozyme–Gd(III)–GlcNAc the hydrogen bond appears somewhat less linear. The reason for this shift is not obvious. The effect is to increase the Gd(III) (aspartic acid-52 site) –O-7 distance from 0.73nm, which it would be in the lysozyme–βMeGlcNAc structure, to 0.83nm. It is worth noting that there appears to be conformational flexibility about the C-2–N-2 bond of acetamido sugars. For example in the crystal structure of *N*-acetylmuramic acid there is considerable inclination of the *N*-acetyl plane [51° compared with 78° in αGlcNAc (Johnson, 1966)] with respect to the best plane of all six sugar-ring atoms (Knox & Murthy, 1974). The inclination of the plane in *N*-acetylmuramic acid results in an intramolecular hydrogen bond to the lactyl carbonyl group.

Co-crystallized lysozyme–Gd(III) derivative

The co-crystallized lysozyme–Gd(III) crystals are tetragonal $P4_32_12$ as deduced from precession photographs, but their external morphology differs from that of native lysozyme. The crystals diffract weakly,

Table 5. *Separation of key atoms at the active site of lysozyme and lysozyme–Gd(III) complexes*

Lysozyme complex	Separation of atoms (nm): Asp-52–Glu-35 carboxy C atoms	Glu-35 carboxy C atom–Trp-108 $N^{\varepsilon 1}$ atom
RS5D co-ordinates of native lysozyme	0.70	0.54
Lysozyme–Gd(III)	0.67	0.52
Lysozyme–Gd(III)–GlcNAc	0.68	0.52

Table 6. *Comparison of distances in nm of the Gd(III) sites in the tetragonal and triclinic crystal forms of lysozyme*
The pairs of distances given in the Table for tetragonal lysozyme are between the oxygen atoms of each carboxy group and the Gd(III) site in question. For triclinic lysozyme the distance is to the closest oxygen atoms of glutamic acid-35 and aspartic acid-52. Soaking times were 20h for tetragonal lysozyme and 4 weeks for triclinic lysozyme (Kurachi *et al.*, 1975).

Crystal	Gd(1)–Gd(2)	Gd(1)–Glu-35	Gd(2)–Asp-52	Occupancy (%): Site 1	Site 2
Lysozyme–Gd(III) (tetragonal)	0.35	0.46, 0.22	0.40, 0.31	24	38
Lysozyme–Gd(III)–GlcNAc (tetragonal)	0.38	0.47, 0.26	0.36, 0.25	23	38
Lysozyme–Gd(III) (triclinic)	0.36	0.25	0.31	3.6	1.6

giving very different photographs to those for the diffused lysozyme–Gd(III) crystals. The unit-cell dimensions were found to be $a = b = 8.08$ nm and $c = 3.54$ nm, and differ considerably from $a = b = 7.91$ nm and $c = 3.79$ nm for native lysozyme. The unit-cell volumes are similar at 231 and 237 nm^3 respectively. Co-crystallization of lysozyme with praseodymium salts yields crystals that are isomorphous with those for native lysozyme (R. Cassels, personal communication).

Discussion

Physical significance of the lysozyme–Gd(III) binding

In the tetragonal crystal form of lysozyme, Gd(III) is observed to bind the two sites 0.36 nm apart, one of which is close to aspartic acid-52 and the other close to glutamic acid-35.

The positions of the gadolinium sites are similar to those observed in triclinic lysozyme (Table 6). The occupancies are an order of magnitude higher and in reverse order in the tetragonal studies. This is remarkable in view of the 1:23 difference in soaking times used. The differences in occupancies may be the results of the intermolecular packing in the tetragonal and triclinic forms, which also appears to bring about other differences. For example, the binding of αGlcNAc in subsite C-α is not observed in triclinic crystals of lysozyme GlcNAc (Kurachi *et al.*, 1976). The occupancies in the present study are consistent with the state of ionization of the two carboxy groups at pH 4.7 as predicted from their macroscopic pK values [aspartic acid-52, p$K = 3.4$; glutamic acid-35, p$K = 6.0$ (Imoto *et al.*, 1972; Kuramitsu *et al.*, 1974)].

In the tetragonal crystal form there are two arginine residues (at positions 21 and 125) whose side chains come close to the glutamic acid-35 and aspartic acid-52 carboxy side chains in a symmetry-related molecule, although the distances for arginine-125 are greater than 1.0 nm. The proximity of these positively charged groups in the crystal lattice might affect the binding of gadolinium and explain the differences observed in the cell dimensions of the co-crystallized lysozyme–Gd(III) complex. However, the closest approach of the guanidinium group of the symmetry-related arginine-21 residue is 0.58 nm [between site Gd(2) and the $N^{\eta 2}$ atom of arginine-21]. The distances between arginine-21 and site Gd(1) are greater than 0.63 nm, and the distances between arginine-21 and the carboxy groups of glutamic acid-35 and aspartic acid-52 are considerably greater than 0.6 nm. Thus arginine-21 interacts very weakly, if at all, with the bound Gd(III) and the carboxy groups of glutamic acid-35 and aspartic acid-52. The close similarity of the metal co-ordinates in the tetragonal and triclinic crystalline forms of lysozyme–Gd(III) complexes implies that the structure of the complex is determined by the protein tertiary structure and not by the constraints of the two different crystal lattices.

The Gd(III) cation cannot bind simultaneously in both sites. The ionic radius of the cation is 0.099 nm (Phillips & Williams, 1966), which on comparison with the separation of about 0.36 nm suggests that the repulsive energy of at least two bivalent positive charges on each cation (after accounting for the charge of the two carboxy groups) would be too great to permit simultaneous binding in the two sites. This interpretation is consistent with the solution studies, which show that a 1:1 complex is formed (Secemski & Lienhard, 1974; Dobson & Williams, 1977).

The crystallographic results (Table 6 and Fig. 2) show that the binding of Gd(III) to the carboxy groups of aspartic acid-52 and glutamic acid-35 is monodentate. Solvent exposures (Shrake & Rupley, 1973) are consistent with this picture, since only one of the two oxygen atoms of both carboxy groups appears to be open to solvent in the native protein. Levine *et al.* (1974) and Levine & Williams (1975) have shown that the lanthanides form bidentate complexes with compounds containing carboxy groups, with an exceptional case being thulium, which forms monodentate complexes, probably as a result of its hydration properties. It appears that the monodentate binding of Gd(III) to lysozyme is unusual and is brought about by the protein tertiary structure. This situation is not unique to lysozyme: a similar double site has been reported for the heavy-atom derivative of crystalline bovine trypsin with Tl^+ in the specificity 'pocket' of trypsin (Stroud *et al.*, 1974).

In view of the proximity of the two carboxy groups at the active site of lysozyme, it might be expected that Gd(III) would form a double bidentate complex at a single site involving the carboxy groups of both glutamic acid-35 and aspartic acid-52. Such a site would require the separations of oxygen atoms between the two carboxy groups to be between 0.44 and 0.48 nm. The separations as measured in the crystal structures are 0.55 nm in the native lysozyme (RS5D co-ordinates) and 0.53 nm in lysozyme–Gd(III)–GlcNAc. Although these separations show that the single site half-way between the two carboxy groups is just possible, the metal cannot occupy such a site without coming within the van der Waals radius of the C^β atom of glutamine-57 (Fig. 2), a residue that is fairly rigidly located in the protein structure. Thus the protein structure appears to forbid a single-site bidentate complex, since the metal is obliged to move away from the line joining the two carboxy groups, increasing one of the metal–oxygen atom distances. Hence the metal appears to make a choice between the two carboxy groups that in the crystal structure results in approx. 38% occupancy

at the aspartic acid-52 site and 23% occupancy at the glutamic acid-35 site.

It is also noteworthy that the main-chain atoms of residues aspartic acid-52 and glutamic acid-35 are relatively firmly located. Aspartic acid-52 is part of the β-pleated sheet that forms the left-hand side of the cleft, and glutamic acid-35 is part of the α-helix that runs through the centre of the right-hand side of the molecule. The side chains have low solvent accessibility, and aspartic acid-52 is involved in hydrogen bonds to asparagine-46 and asparagine-59 in the native protein. Although small shifts in these residues are seen in the present study, the relative immobility of these groups provides a rationalization of the two mutually exclusive Gd(III) sites, since the movement to permit the carboxy group of aspartic acid-52 (for example) to participate in the binding of Gd(III) at the glutamic acid-35 site would be about 0.3–0.4 nm. This comparatively large movement could not be accomplished without disruption of the protein molecule. The apparent inflexibility of these side chains (i.e. movements of 0.03–0.05 nm) may also be relevant to the catalytic mechanism.

There is no evidence from our studies that binding to any of the remaining carboxy groups of lysozyme occurs, although two or more weak binding sites in solution at aspartic acid-101 and at aspartic acid-87 and/or glutamic acid-7 have been reported (Campbell *et al.*, 1975).

Table 7 gives two independent estimations of exposure ratios for the 12 carboxy groups of lysozyme, with a summary of their environments. Only one (glutamic acid-7) is significantly influenced by the intermolecular lattice contacts. It may be thought that, all other things being equal, the binding to weak sites would be preferentially directed towards these carboxy groups with large exposure ratios and not close to any basic residues.

Comparison with solution studies

The crystallographic evidence for two mutually exclusive binding sites for Gd(III) is consistent with the 1:1 stoicheiometry of binding for the lanthanide–lysozyme complexes as concluded from solution studies (Secemski & Lienhard, 1974; Dobson & Williams, 1977).

Comparison of the binding constants for lanthanides to acetic acid, malonic acid and lysozyme (Dobson & Levine, 1976) shows that lysozyme is intermediate in behaviour between acetic acid and malonic acid. This behaviour is consistent with the model proposed from crystallographic evidence.

In an n.m.r. study of exchangeable hydrogen atoms in lysozyme, Campbell *et al.* (1975) observed that the chemical shifts of the resonances assigned to protons of tryptophan-108 were strongly dependent on pH. The pH-dependence of these shifts resulted from ionization of glutamic acid-35 and aspartic acid-52, and it was suggested that on ionization the carboxy group of glutamic acid-35 moves away from tryptophan-108, producing a decrease in the through-space shielding of the carboxy group of glutamic acid-35. Similar shifts to those observed on changing pH were also observed on the binding of La(III) to lysozyme and were explained in terms of competition between a proton and La(III) for the glutamic acid-35 carboxy group, resulting in a decrease in the apparent pK_a value of glutamic acid-35 from 6.0 to 4.2. The relative movement seen in the crystal structure between the $N^{\varepsilon 1}$ atom of tryptophan-108 and the carboxy carbon atom of glutamic acid-35 on binding Gd(III) is 0.02 nm. Thus, although little confidence can be placed in the absolute value of this movement, it appears that there is a small change in the relative separation of these atoms in the crystal structure. If it is assumed that the behaviour in the crystal is the

Table 7. *Accessibilities of the carboxy groups of lysozyme to solvent in the free state*

Only the aspartic acid-52–glutamic acid-35 pair of carboxy groups is within a 0.6 nm separation; there are basic side chains (*) within 0.6 nm of aspartic acid-66, aspartic acid-18, aspartic acid-48, aspartic acid-87 and α-CO_2H (Imoto *et al.*, 1972). Only the side chain of glutamic acid-7 is obstructed by lattice contracts (by about 50%) on incorporation of lysozyme into the crystal lattice (Shrake & Rupley, 1973).

	Exposure ratio	
Carboxy group	After Imoto *et al.* (1972)	After Shrake & Rupley (1973)
Asp-66*	0.0	0.0
Glu-35	0.2	0.2
Asp-18*	0.3	0.3
Asp-48*	0.3	0.4
Asp-52	0.3	0.3
Glu-7*	0.4	0.4
Asp-119	0.5	0.4
Asp-87*	0.7	0.7
α-CO_2H*	0.7	0.7
Asp-101	0.8	0.9

same as that in solution (an assumption that may not be justified in detail), then these results provide a measure of sensitivity of n.m.r. methods for the detection of conformational changes.

From solution studies on hen lysozyme, pK 6.0–6.5 has been assigned to glutamic acid-35 and pK 3.5 to aspartic acid-52 (Imoto *et al.*, 1972; Rupley *et al.*, 1974). There is some evidence from circular-dichroism studies (Kuramitsu *et al.*, 1974) that the properties of the two carboxy groups are interrelated and that the electrostatic interaction with aspartic acid-52 contributes to the high pK of glutamic acid-35. This view is supported by n.m.r. studies (Dobson & Williams, 1977). It seems likely that the carboxy groups of aspartic acid-52 and glutamic acid-35 must both participate in the binding of lanthanides in solution in order to rationalize the existence of the major binding site there in the protein. The binding is associated with a pK of about 4 in the n.m.r. experiments, and no further end points are observed at higher pH (Dobson & Williams, 1977). From the shift-dependence of the tryptophan-108 n.m.r. signals, it was concluded that glutamic acid-35 is implicated in the binding process, although no firm conclusions were stated on the involvement of aspartic acid-52 in the binding of lanthanide (Dobson & Williams, 1977). The lanthanide-induced shift ratios are constant over the pH range, and it was deduced that a single binding mode of lanthanides to lysozyme occurs in solution. The distinction between one or two binding sites in solution and the precise correlation between the crystal and solution studies must await further experiments.

Recently the one-position and two-position Gd(III) models have been analysed with respect to the n.m.r. data for the sugar inhibitor binding to lysozyme–lanthanide complexes (S. J. Perkins & R. A. Dwek, unpublished work). The agreements between the observed and calculated shifts for the sugar protons are similar for both models, and hence, on this basis, the n.m.r. studies cannot distinguish between the one-site and the two-site model.

The overall physical picture that emerges from the crystallographic studies for lanthanides may be described as follows. Provided that aspartic acid-52 is ionized in the uncomplexed protein, the lanthanide cation senses this on a similar basis to the other single ionized carboxy groups and binds weakly to it. However, on binding to aspartic acid-52, the lanthanide also senses the presence of the glutamic acid-35 carboxy group, albeit protonated, and the initial scene is set for a competition between the doubly charged Gd(III) bound to aspartic acid-52 and the proton of glutamic acid-35. The end result is the rapid exchange of the metal cation between the two extreme positions at the two carboxy groups and the ejection of the proton. At present, a fuller understanding of the processes involved at the catalytic site of lysozyme is hindered by the lack of experience with models based on this type of system.

S. J. P. acknowledges support from the Medical Research Council. This is a contribution from the Oxford Enzyme Group. We are grateful to Dr. K. W. Snape for help with the data processing, to Miss D. E. P. Grace for generously making available phases calculated in the seventh cycle of the crystallographic refinement of tetragonal lysozyme and to Dr. R. A. Dwek for discussions on the n.m.r. studies.

References

Agresti, D. G., Lenkinski, E. E. & Glickson, J. D. (1977) *Biochim. Biophys. Res. Commun.* **76**, 711–719

Arndt, U. W., North, A. C. T. & Phillips, D. C. (1964) *J. Sci. Instrum.* **41**, 421–425

Blake, C. C. F., Koenig, D. F., Mair, G. A., North, A. C. T., Phillips, D. C. & Sarma, V. R. (1965) *Nature (London)* **206**, 757–761

Blundell, T. & Johnson, L. N. (1976) *Protein Crystallography*, Academic Press, London

Campbell, I. D., Dobson, C. M. & Williams, R. J. P. (1975) *Proc. R. Soc. London Ser. A.* **345**, 41–59

Diamond, R. (1971) *Acta Crystallogr. Sect. A.* **27**, 436–452

Diamond, R. (1974) *J. Mol. Biol.* **82**, 371–391

Dobson, C. M. & Levine, B. A. (1976) in *New Techniques in Biophysics and Cell Biology*, (Pain, R. H. & Smith, B. J., eds.), vol. 3, pp. 19–91, Wiley, London

Dobson, C. M. & Williams, R. J. P. (1977) in *Metal–Ligand Interactions in Organic Chemistry and Biochemistry* (Pullman, B. & Goldblum, N., eds.), part 1, pp. 255–282, Reidel, Dordrecht

Dwek, R. A. (1973) *NMR in Biochemistry*, Oxford University Press, Oxford

Dwek, R. A., Richards, R. E., Morallee, K. G., Nieboer, E., Williams, R. J. P. & Xavier, A. V. (1971) *Eur. J. Biochem.* **21**, 204–209

Dwek, R. A., Morallee, K. G., Nieboer, E., Richards, R. E., Williams, R. J. P. & Xavier, A. V. (1973) *Proc. Rare Earth Res. Conf. 10th* 111–116

Hamilton, W. C., Rollett, J. S. & Sparks, R. A. C. (1965) *Acta Crystallogr.* **18**, 129–130

Imoto, T., Johnson, L. N., North, A. C. T., Phillips, D. C. & Rupley, J. A. (1972) *Enzymes 3rd Ed.* **7**, 665–868

Johnson, L. N. (1966) *Acta Crystallogr.* **21**, 885–891

Jones, R., Dwek, R. A. & Forser, S. (1974) *Eur. J. Biochem.* **47**, 271–283

Knox, J. R. & Murthy, N. S. (1974) *Acta Crystallogr. Sect. D* **30**, 365–371

Kurachi, K., Sieker, L. C. & Jensen, L. H. (1975) *J. Biol. Chem.* **250**, 7663–7667

Kurachi, K., Sieker, L. C. & Jensen, L. H. (1976) *J. Mol. Biol.* **101**, 11–24

Kuramitsu, S., Ikeda, K., Hamaguchi, K., Fujio, H., Amaro, T., Mina, S. & Nishua, T. (1974) *J. Biochem. (Tokyo)* **76**, 671–683

Lenkinski, R. E., Agresti, D. G., Chen, D. M. & Glickson, J. D. (1978) *Biochemistry* **17**, 1463–1468

Levine, B. A. & Williams, R. J. P. (1975) *Proc. R. Soc. London Ser. A* **345**, 5–22

Levine, B. A., Thornton, J. M. & Williams, R. J. P. (1974) *J. Chem. Soc. Chem. Commun.* 669–670
North, A. C. T. (1965) *Acta Crystallogr.* **18**, 212–216
North, A. C. T., Phillips, D. C. & Mathews, F. S. (1968) *Acta Crystallogr. Sect. A* **24**, 351–359
Perkins, S. J. (1977) D.Phil. Thesis, University of Oxford
Perkins, S. J., Johnson, L. N., Phillips, D. C. & Dwek, R. A. (1976) *Int. Conf. Magnetic Resonance in Biological Systems 7th, St. Jovite, Canada*, Abstract TH-P27
Perkins, S. J., Johnson, L. N., Machin, P. A. & Phillips, D. C. (1978) *Biochem. J.* **173**, 607–617
Phillips, C. G. S. & Williams, R. J. P. (1966) *Inorganic Chemistry*, Oxford University Press, Oxford
Phillips, D. C. (1964) *J. Sci. Instrum.* **41**, 123–129
Rupley, J. A., Bannerjee, S. K., Kregan, I., Lepanje, S., Shrake, A. F. & Turk, V. (1974) in *Lysozyme* (Osserman, E. F., Canfield, R. E. & Beychok, S., eds.), pp. 251–268, Academic Press, New York and London
Secemski, I. I. & Lienhard, G. E. (1974) *J. Biol. Chem.* **249**, 2932–2938
Shrake, A. & Rupley, J. A. (1973) *J. Mol. Biol.* **79**, 351–371
Stroud, R. M., Kay, L. M. & Dickerson, R. E. (1974) *J. Mol. Biol.* **83**, 185–208
Teichberg, V. I., Sharon, N., Moult, J., Somalsky, A. & Yonath, A. (1974) *J. Mol. Biol.* **87**, 357–368